

Systems Adaptation for Satellite Signal under Dust, Sand and Gaseous Attenuations

Kamal Harb*, Omair Butt, Samir Abdul-Jauwad, Abdulaziz M. Al-Yami

Electrical Engineering Department, KFUPM University, Dhahran 31261, Saudi Arabia

Abstract Sand, dust, gaseous and other atmospheric properties have a distorting effect on signal fidelity of Ku and Ka bands. Such distributions result in signal transmission error commensuration with different weather attenuations. These attenuations severely affect quality of service (QoS) as well as service level agreement (SLA). The main focus of this paper is to propose a new model for atmospheric impairments affecting satellite communication networks that operate at high frequencies. These operations are heavily dependent on the propagation characteristics in desert areas, due to the often occurring of dust and sand storms as well as gaseous attenuations. Furthermore, gaseous attenuation (GA) can be estimated by using predicted signal-weather correlated database in collaboration with ITU-R propagation models combined with interpolation methods, gateway, and ground terminal characteristics. A three dimensional relationship is then proposed for these attenuations with visibility, dust particular size, frequency, and propagation angle to provide decision and control system (DACS) with an enhanced view of satellite performance. This system is controlled by a skilful atmospheric aware model (SAAM) that can enable mitigation planning by adaptively selecting satellite parameters to improve network performance and monitor receiving signal to maintain the predefined threshold level under different weather conditions. Simulation results are presented to show the effectiveness of the proposed scheme.

Keywords Decision and Control System, Dust and Sand Storms, Gaseous Attenuation, International Telecommunication Union Radio Communications, Quality of Service, Satellite Networks, Signal to Noise Ratio, Skilful Atmospheric Aware Model, Visibility

1. Introduction

The rapid growth of wireless and satellite networks for communication on Ku and Ka bands have been widely employed. However, propagation impairments due to atmospheric attenuations can cause uncontrolled variations in signal level, phase, polarization, and angle of arrival. This will result in excessive digital transmission errors. These propagation impairments differ from one location to another on earth and are presented by dust, sand and gaseous attenuations in areas like Saudi Arabia. These attenuations become particularly severe at frequencies higher than 10 GHz, especially for very small aperture terminal (VSAT) [1]-[3].

Dust and sand attenuations (DASA) are considered a dominant impairment for satellite signals in the desert area. Fig. 1 shows an extreme sand and dust storm formation [4].

Thus quality of service (QoS) in satellite networks are severely affected while facing these kinds of atmospheric conditions.

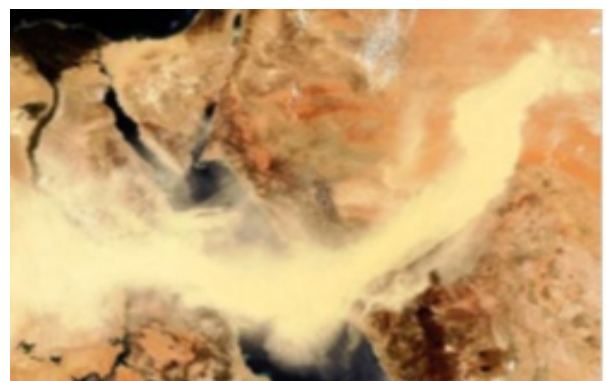


Figure 1. Sand and dust storms formation in Western Region

Knowing the atmospheric characteristics are important factors for system reliability and QoS provisioning in satellite networks. International Telecommunication Union Radio Communications (ITU-R) maintains a database for atmospheric characteristics around the world that is used to estimate weather attenuations and other parameters. This attenuation is based on the concept of deriving the effective length of path through different weather conditions. The

* Corresponding author:

kharb@kfupm.edu.sa (Kamal Harb)¹

Published online at <http://journal.sapub.org/jwnc>

Copyright © 2013 Scientific & Academic Publishing. All Rights Reserved

¹ "This work is supported by the Deanship of Scientific Research (DSR) at King Fahd University of Petroleum & Minerals (KFUPM) through project No. FT121013".

effective path in this paper takes into account the spatial non-uniformity of dust, sand, gaseous, and other atmospheric conditions, both horizontally and vertically [5],[6].

Although some work has been done to study the impact of weather characteristics in satellite networks, most of the existing work considers uniform dust particular size distribution within the storm and/or low elevation angle cases only. In [7], the authors presented the prediction models and the analytical techniques for a range of operational parameters involving low-margin, low elevation angle, inclined geosynchronous, and low earth orbit systems that are applied to the areas of VSAT systems, traditional communications, mobile, and personal communications applications[8].

A number of papers[9]-[20] have presented this phenomenon. The behavioural and compositional characteristics of dust and sand storms from different areas of world are uncorrelated due to variant regions and weather specific factors. The impacts of dust storms become more significant for signals having shorter wavelengths which observe more attenuation and scattering from particles of sand and dust in the radio path. In [16] the phenomenon of vertical variation of visibility was discussed. In [20], another approach for adding a vertical path adjustment factor to measure attenuation is presented. This paper generalizes the concepts of [11],[16],[20]-[24], and present a three dimensional relationship for average dust particle size variations with respect to different reference visibilities, dust particular size, and heights. Thus, the method to get enhanced attenuation and signal to noise ratio (SNR) measures have been presented based on the mentioned parameters. This scheme for modelling, estimating and proposing, would be helpful in optimizing the radio resources and implementing the cost effective link budgets for satellite links while maintaining the end-to-end QoS requirements.

This paper introduces a novel method to enhance ITU-R

models by improving its computational efficiency and prediction accuracy for different atmospheric parameters based on weather database at different sites and frequencies. In addition, a three dimensional relationship is proposed for atmospheric attenuations with visibility, particle size, frequency and propagation angle. These results will supply the proposed skilful atmospheric aware model (SAAM) with a mechanism to better estimate satellite networking parameters such as link and queuing characteristics. These derived parameters will then enable the adaptive SAAM to maintain QoS and service level agreements (SLAs) by adaptively adjusting signal power, channel rate, location, propagation angle, frequency, coding, and modulation schemes under fierce weather conditions. Moreover, this proposed method can be used to build up a flexible system based on optimized algorithm and core computing skillful model which takes into account challenging propagation environments and the need to extend deterministic models to predict parameters relevant to the communication system simulation. Consequently, it will promptly adjust to new signal fluctuations through the inter-connected network entities before storm weather effect actually manifest themselves to maintain end-to-end bit error rate (BER) requirements[6]-[8],[25]. Simulation results for SNR with both the estimated attenuations and the transmit power, are presented to show the performance improvements. The remaining sections of this paper are as follows:

Section 2 introduces the atmospheric attenuations impact on satellite communications. Section 3 presents QoS in weather impacted satellite networks followed by a simulation and analysis of atmospheric attenuations. In Section 4, skilful atmospheric aware model (SAAM) for satellite systems are presented. Section 5 presents simulation results and discussions. Finally, the conclusion is presented in Section 6.

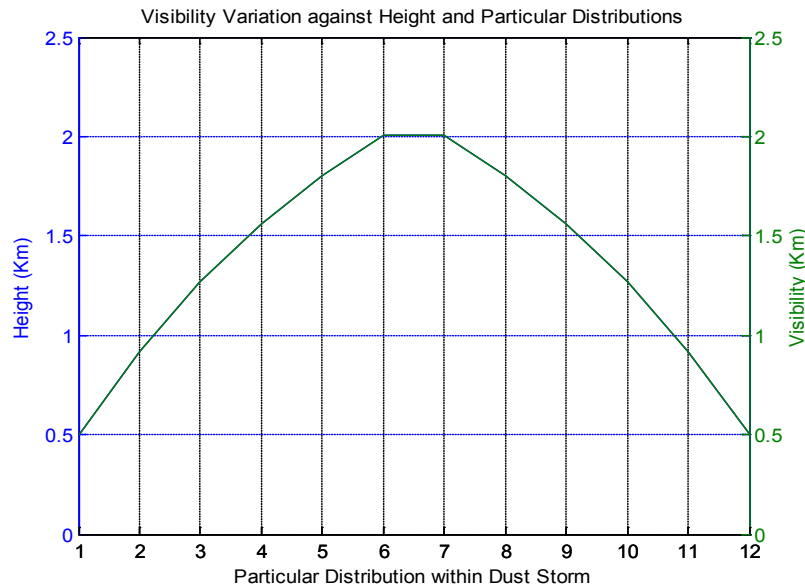


Figure 2. Visibility variation of dust storm according to different height

2. Atmospheric Attenuations Impact on Satellite Communications

This section introduces dust, sand, and gaseous attenuations and their impact on satellite communications.

2.1. Dust and Sand Storms Presentation

Dust and sand storms are very common meteorological phenomenon being observed in desert and dry areas such as Saudi Arabia, Arizona, Sudan, Iraq, Libya, etc. Usually, these storms arise due to strong winds causing the dust particles to get suspended in the atmosphere. These storms have varying maximum altitude depending upon specific regional characteristics and wind blow speeds.

Severity of dust storms depends upon the visibility, or in other words the intensity of dust storms increases as the visibility decreases. Dust storms can attain altitudes of 5 km or more in the atmosphere[19]. An approach to model these storms and methods to get enhanced attenuation measurements is presented in this paper based on the knowledge of two dimensional (side and top view) models of dust storms as discussed in[20]-[22].

2.1.1. Concept of Dust Storm Layers

The intensity of dust storm is not uniformly distributed and it varies both horizontally and vertically with the highest in the middle and lowering around the horizontal start, end and vertical edges. It contains several layers while moving from the base, in vertical direction, to the top. These layers represent different levels of visibility based on non-uniform particle size and intensity distributions within the DASA as shown in Fig. 2. This figure displays the dust storm for different height layers and visibilities. Thus, the visibility increases to its maximum at the highest level of dust storm. The results were acquired for up to 2 km in dust storms' altitude along with different estimated visibilities. Such as, for 1.8 km of visibility, the height will be equal to 1.2 km. The physical representation of dust storm according to visibility variations with different levels shall lead to an improved estimation of weather attenuation. The results are of significant achievement.

Therefore, the particle size distribution is similar to an exponentially decaying function, where the base layer contains heavier and denser particles leading to more attenuation. However, by moving in lateral direction, the size and density of the particles shall reduce, which constitute lesser attenuation. Note that, the line at the center of the figure divides the dust storm into two similar phases. Therefore, accurate estimation of dust storm height leads to better estimation of the channel attenuation which in turn, saves extra transmission power and improves QoS. These storms present the major cause of attenuation on satellite communication channels. DASA analysis and results will be presented in section 3.1.

Thus, wireless channels are susceptible to several impairments simultaneously, including several weather anomalies. The following section covers gaseous

presentation.

2.2. Gaseous Presentation

As signal passes through the troposphere, they undergo interactions with the gas molecules that are present in the atmosphere. The atmosphere composition being at sea level includes: Nitrogen (N_2) = 78%, oxygen (O_2) = 21%, and the remaining of around 1% are represented by argon (Ar), carbon dioxide (CO_2) which varies with location, neon, helium, krypton and water vapour (H_2O) which varies in concentration from 0 to 2%, with trace quantities of: methane (CH_4), sulphur dioxide (SO_2), ozone (O_3), nitrogen oxide (NO), and nitrogen dioxide (NO_2)[26],[27].

Each of these gas molecules interact with the propagated signal. The interactions may or may not cause loss of energy and hence attenuation. Losses are especially high near the resonances of the molecules as presented in the following sections. Such as, when an asymmetric molecule (e.g., H_2O) is placed in an electric field, it will try to align itself to minimum potential with respect to the electric field. Some of the important factors to remember are that absorption depends mainly on:

- The resonant frequency of gas molecules
- The concentration of that gas in the atmosphere
- The path length.

Besides that, the atmospheric pressure is important. The resonance modes of the molecules are discrete. Since the molecules are constantly in collision with each other and moving at random, the resonance lines become broadened. Notice that, below 10 GHz, gaseous attenuation (GA) can be ignored for most purposes.

The important resonances for gaseous absorption up to 300 GHz are those from atmospheric oxygen and water vapour.

The quantities and effects of resonant gases (CO , NO , NO_2 , N_2O , SO_2 , O_3) are negligible compared to water vapour at typical microwave link frequencies.

Oxygen has strong bands of resonances around 57 – 60 GHz and 119 GHz. At sea level, the losses can mount up to 15 dB/km at between 57 GHz and 63 GHz. Satellite network designers should be aware of transmission signal with carrier frequencies around 22 GHz, 183 GHz, and 324 GHz because water vapour has resonance which increases the gaseous attenuation effect to the maximum. The attenuation changes with the amount of water vapour in the atmosphere. GA analysis and results will be discussed in section 3.2[3], [26]-[27].

3. QoS in Weather Impacted Satellite Networks

Weather conditions have little to no effect upon low operational frequencies. However, QoS of a satellite network is hardly affected by atmospheric attenuations at reasonably high transmission frequency. This section proposes a new method for calculating dust and sand attenuations based on

different layers that contain various visibility and dust storm particular size distributions. The gaseous attenuation model is achieved by implementing an updated adaptive software that uses ITU-R data for this attenuation combined with bi-linear interpolation[29] at any location on earth, for a wide range of satellite parameters as per[1]-[3],[23].

3.1. Analysis and Simulation for Dust and Sand Attenuations in 3-D

The proposed dust storm formation will be chopped off into multiple layers based on the concept of doubling visibility from the starting point of each layer[23]. To achieve more precision, the visibility window should be narrower, but this precision might affect the computational cost while consuming additional layers. Expression (1) can be used in a recursive manner to obtain the visibility based layers in dust storm:

$$h_l = h_{(l-1)} \left[\frac{V_l}{V_{(l-1)}} \right]^{-0.26}, \quad (1)$$

where $h_{(l-1)}$ and $V_{(l-1)}$ are the reference height and visibility respectively, and the suffix (l) indicates different dust layers. Equation (1) can be modified to find various levels of visibility depending upon different heights:

$$V_l = V_0 \left[\frac{h_l}{h_{(l-1)}} \right]^{0.26}. \quad (2)$$

Similarly, by generalizing the concept of[20],[23] the total slant path (L) traversed by microwave signal in the dust storm is broken into smaller patches based on different levels of visibility at each layer, as follows:

$$L(\theta) = L_1 + L_2 + \dots + L_N = \sum_l^N \frac{h_l}{\sin\theta} \quad (3)$$

3.1.1. Non-Uniform Dust Distribution

Dust particle size distribution assessment is very important for predicting effects of dust storms. Each dust storm may have totally uncorrelated dust distributions. Moreover, this distribution is also dependent on height. As the height decreases, the particles average diameter increases because the heavier dust particles have greater fall velocities as compared to the particles with smaller sizes that remain suspended in the air for longer intervals of time. For all the samples, the relation between average diameter D_{av} (μm) and height h (m) can be represented by[20]:

$$D_{av} = D_0 h^{-\alpha}, \quad (4)$$

where, $\alpha = 0.155$ by combining (1) and (4).

To assume an approximate circular geometry for the dust particles, the equivalent or average dust particles sizes are computed as:

$$R_{eq} = D_{av} / 2. \quad (5)$$

After mathematical manipulation another expression is presented for computing the values of average diameter of dust particles at several reference heights and visibilities[23]:

$$D_{av}(h, V_l) = \left[\frac{D_0}{h_0} \right] \left[\frac{V_l}{V_0} \right]^{0.0403}, \quad (6)$$

where the visibility V_l is in km at level l , while D_0 , h_0 and V_0 are reference diameter, height, and visibility, respectively.

For this computation, Freeman's chain code algorithm was incorporated for averaging the dustparticle in many sizes for better estimates. This estimation provides an enhanced result under light andmedium dust storms, where the dust particle size is assumed to be uniformly distributed. Therefore, in caseof heavy dust storm scenario other assumptions should be presented to achieve reasonable outcome.

3.1.2. Dust Attenuation Modeling

Each layer constitutes its specific point of attenuation at the microwave signal depending on the measureof visibility as well as the equivalent dust particle radii. These individual layered attenuations are then summed up to reach the end of dust storm which can be discovered by attaining certain lower bound ofvisibility when compared to visibility in free space[9],[17],[22],[23]. The point attenuation is presented as follows:

$$A_{pi} = \left[\frac{567}{VR_{eq}^2 \lambda} \right] \left[\frac{\epsilon''}{(\epsilon' + 2)^2 + \epsilon''^2} \right] \sum_i P_i r_i^3 \quad (7)$$

Where $\sum_i P_i r_i^3$ represents the summation for different probabilities of particle sizes multiplied by the cubicoof the dust particle size. The outcome of (7) is shown in Fig. 3. A lso, listing values of dielectric constants at various frequencies is measured by[15],[23],[31].

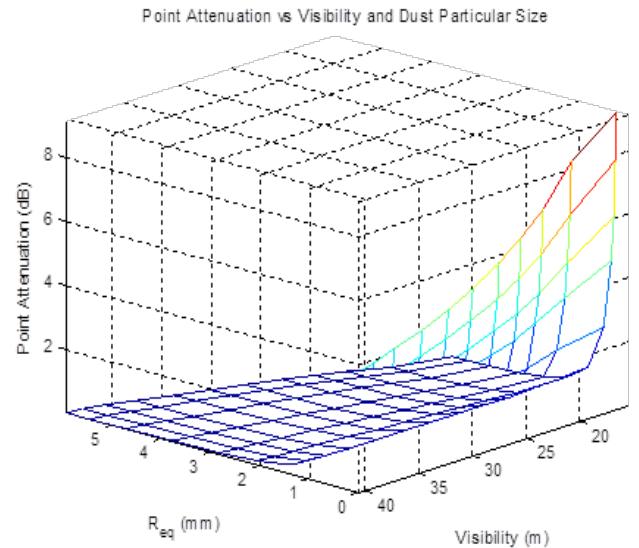


Figure 3. Point attenuation with particles radius and visibility

By combining (1) through (7), the total dust and sand attenuation along the path as a function of frequency and propagation angle with different particular sizes can be presented as follows:

$$A_{DASA}(\theta, f) = \sum_l^N \left[\frac{567 \times f}{V(\theta) R_l^2 c} \right] \left[\frac{\epsilon''}{(\epsilon' + 2)^2 + \epsilon''^2} \right] \sum_i^n P_i r_i^3. \quad (8)$$

Thus, the dust particular radius (R_l) decreases monotonically while moving up across the dust layers. Theproposed model takes into account the range of visibilities with several sizes forboth dust and sand

particles along with altitude dependent distributions, to compute their respective attenuations for a wide range of frequencies and propagation angles as shown in Fig. 4.

3.2. Analysis and Simulation for Gaseous Attenuation (GA)

In this section, analytical solution for GA is presented. Thus, predicting GA requires a model that allows us to represent the specific attenuation mathematically. It can be calculated by summing the effects of all of the significant resonance lines given in [26] as:

1- Specific Attenuation:

A- For dry air, the attenuation $\gamma_0(f)$ (dB/km) for the frequency ($f \leq 54$ GHz) is:

$$\gamma_0(f) = \left\{ \frac{7.2r_t^{2.8}}{f^2 + 0.34r_{ph}^2 r_t^{1.6}} + \dots \right. \\ \left. \dots + \frac{0.62\xi_3}{(54-f)^{1.16\xi_1 + 0.83\xi_2}} \right\} \cdot f^2 \cdot r_{ph}^2 \cdot 10^{-3} \quad (9)$$

with

$$\xi_1 = \varphi(r_{ph}, r_t, 0.0717, -1.8132, 0.0156, -1.6515), \quad (10)$$

$$\xi_2 = \varphi(r_{ph}, r_t, 0.5146, -4.6368, -0.1921, -5.7416) \quad (11)$$

and

$$\xi_3 = \varphi(r_{ph}, r_t, 0.3414, -6.5851, 0.2130, -8.5854) \quad (12)$$

$$\varphi(r_{ph}, r_t, a, b, c, d) = r_{ph}^a \cdot r_t^b \cdot \exp[c(1 - r_{ph})] + d(1 - r_t) \quad (13)$$

B- For water vapor, the attenuation $\gamma_w(f)$ (dB/km) for different frequency ranges is expressed by:

$$\gamma_w(f) = \left\{ \begin{aligned} & \frac{3.98\eta_1 \exp[2.23(1-r_t)]}{(f-22.235)^2 + 9.42\eta_1^2} g(f, 22) + \dots \\ & \dots + \frac{11.96\eta_1 \exp[0.7(1-r_t)]}{(f-183.31)^2 + 11.14\eta_1^2} + \dots \\ & \dots + \frac{0.081\eta_1 \exp[6.44(1-r_t)]}{(f-321.226)^2 + 6.29\eta_1^2} + \dots \\ & \dots + \frac{3.66\eta_1 \exp[1.6(1-r_t)]}{(f-325.153)^2 + 9.22\eta_1^2} + \dots \\ & \dots + \frac{25.37\eta_1 \exp[1.09(1-r_t)]}{(f-380)^2} + \dots \\ & \dots + \frac{17.4\eta_1 \exp[1.46(1-r_t)]}{(f-448)^2} + \dots \\ & \dots + \frac{844.6\eta_1 \exp[0.17(1-r_t)]}{(f-557)^2} g(f, 557) + \dots \\ & \dots + \frac{290\eta_1 \exp[0.41(1-r_t)]}{(f-752)^2} g(f, 752) \end{aligned} \right\} \quad (14)$$

With

$$\eta_1 = 0.955 \cdot r_{ph} \cdot r_t^{0.68} + 0.006 \cdot \rho, \\ \eta_2 = 0.735 \cdot r_{ph} \cdot r_t^{0.5} + 0.0353 \cdot r_{ph}^4 \cdot \rho \quad (15)$$

and

$$g(f, f_i)A = 1 + \left(\frac{f-f_i}{f+f_i} \right)^2, \quad (16)$$

where ph : pressure (hPa), $r_{ph} = ph/1013$, $r_t = 288/(273 + t)$, ρ : water-vapor density (g/m^3), f : frequency (GHz), and t : mean temperature values ($^{\circ}C$), can be obtained from [26] for most cases.

2- Slant Path Equivalent Height:

The slant path attenuation depends on the distribution along the path of meteorological parameters such

as temperature, pressure, and humidity. Thus, it varies with location, month of the year, height of the station above sea level, and propagation angle.

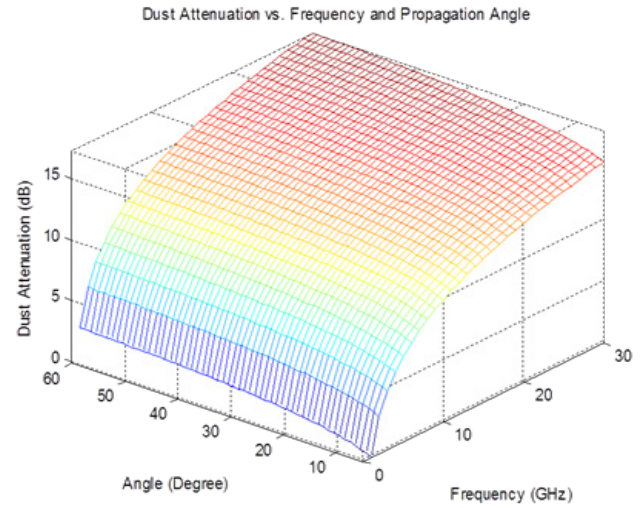


Figure 4. Dust attenuation with frequency and propagation angle

A- For dry air, the equivalent height is given by:

$$h_0(f) = \frac{6.1}{1 + 0.17r_{ph}^{-1.1}} [1 + t_1(f) + t_2(f) + t_3(f)] \quad (17)$$

Where

$$t_1(f) = \frac{4.64}{1 + 0.066r_{ph}^{-2.3}} \cdot \exp \left[- \left(\frac{f-59.7}{2.87 + 12.4 \exp(-7.9r_{ph})} \right)^2 \right] \quad (18)$$

$$t_2(f) = \frac{0.14 \cdot \exp(2.12r_{ph})}{(1-118.75)^2 + 0.031 + 2.2r_{ph}} \quad (19)$$

And

$$t_3(f) = \frac{0.0114}{1 + 0.14r_{ph}^{-2.6}} \cdot \frac{-0.0247 + 10^{-4}f + 1.61 \cdot 10^{-6}f^2}{1 - 0.0169f + 4.1 \cdot 10^{-5}f^2 + 3.2 \cdot 10^{-7}f^3} \quad (20)$$

With the constraint that: $h_0 \leq 10.7$. $r_{ph}^{0.3}$ for $f < 70$ GHz.

B- For water vapor, the equivalent height for $f \leq 350$ GHz is:

$$h_w(f) = 1.66 \cdot \left\{ 1 + \frac{1.39 \cdot \sigma_w}{(f-22.235)^2 + 2.56 \sigma_w} + \frac{3.37 \cdot \sigma_w}{(f-183.31)^2 + 4.69 \sigma_w} + \frac{1.58 \cdot \sigma_w}{(f-325.1)^2 + 2.89 \sigma_w} \right\} km \quad (21)$$

Where

$$\sigma_w = \frac{1.013}{1 + \exp[-8.6(r_{ph} - 0.57)]} \quad (22)$$

Notice that water vapor has resonance of 22.235 GHz, 183.31 GHz, and 325.1 GHz, respectively. Attenuation also changes with the amount of water vapor in the atmosphere.

3- Path Attenuation for Earth-Space propagation angles between 5 and 70 degrees:

The above method calculates slant path attenuation for water vapor that relies on the knowledge of the profile of water-vapor pressure (or density) along the attenuation path. It provides useful general tool for scaling gas according to these parameters. Thus, the approximate gaseous values can

be computed at any desired location, for all range of angles and frequencies as shown in Fig. 5.

Consequently, to obtain the path attenuation based on surface meteorological data using the cosecant law for a given propagation angle and frequency can be obtained as follows:

$$A_G(\theta, f) = \frac{A_0(f) + A_w(f)}{\sin\theta} \text{ dB},$$

where $A_0(f) = h_0(f) \cdot \gamma_0(f) \text{ dB}$,

and

$$A_w(f) = h_w(f) \cdot \gamma_w(f) \text{ dB}. \quad (23)$$

The gaseous attenuation was initially presented by ITU-R, and is expanded in this paper to display its variations with both frequencies and propagation angles. Note that, the elevation angle above 25° has relatively small effect on GA.

Also, Fig. 5 provides designers with a clear view of estimated attenuation for different frequencies that states the maximum level around 22 GHz with low elevation angles.

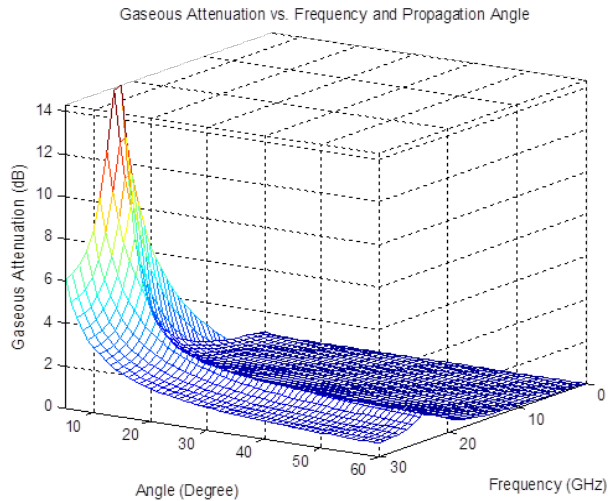


Figure 5. Gaseous attenuation at KFUPM, Dhahran, Saudi Arabia

3.3. Analysis and Simulation for Atmospheric Attenuations

The aim of this section is to estimate different atmospheric attenuations such as sand, dust, and gaseous using predicted signal-weather correlated database in collaboration with ITU-R propagation models combined with interpolation methods, gateway, and ground terminal characteristics.

A three dimensional relationship for these attenuations with respect to propagation angle and frequency is presented in Fig. 6 [1]-[3], [5]. These attenuations, for systems operating at frequencies above 10 GHz — especially those operating with low propagation angles and/or margins, must be considered along with the effect of multiple sources of simultaneous occurring [32].

This method provides a useful general tool for scaling atmospheric attenuations according to these parameters. Also, it helps to provide designers with a perceptible view of approximated different attenuation values that can be computed at any desired location, for different propagation angles, for any probability of precipitation, and for any

specific uplink or downlink frequency.

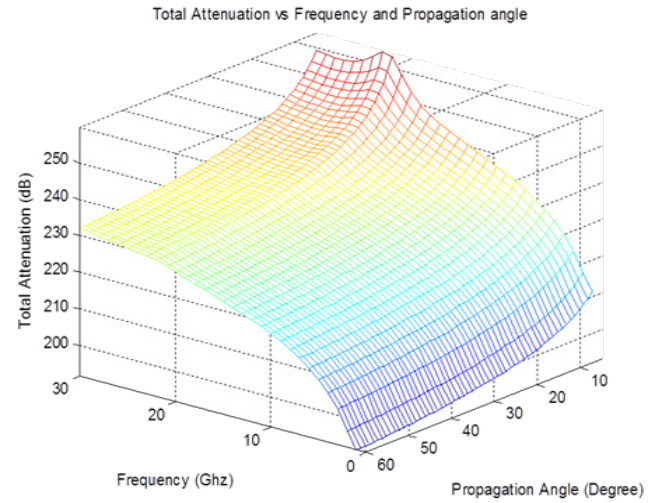


Figure 6. Atmospheric attenuations at KFUPM Station, Dhahran, Saudi Arabia

The outcome becomes a key factor in diagnosing, adjusting and improving satellite signal power, modulation and coding schemes, monitored and controlled altogether by a powerful and efficient skillful – based attenuation countermeasure system. The required input parameters for the above attenuations are:

$A_{DASA}(\theta, f)$: Dust and sand attenuation due to different visibilities, as estimated in (8).

$A_G(\theta, f)$: Gaseous attenuation due to water vapor and oxygen, as estimated in (23).

A general method for calculating atmospheric attenuations $A_w(\theta, f)$, is given by:

$$A_w(\theta, f) = A_{DASA}(\theta, f) + A_G(\theta, f) \quad (24)$$

The results were found to be in good agreement with the available measured data for all latitudes for the prediction of visibilities, dust size, propagation angle, and frequency range as shown in Figs. 4, 5, and 6.

However, due to the dominance of different effects and the inconsistent availability of test data, some variations of errors occur across the distribution of different probabilities.

Thus, knowing this data will be an immense asset to support various analyses for budgeting the operational satellite parameters around the world under severe weather conditions.

4. Skilful Atmospheric Aware Model (SAAM) for Satellite Systems

This section describes different computational techniques to provide decision and control system (DACS) with an enhanced view for modeling satellite propagation environments, and procedures for improving accuracy for the atmospheric attenuations with SNR calculations using different methods.

4.1. Role of Skilful Atmospheric Aware Model (SAAM)

A SAAM has to perceive its environment, to act rationally toward its assigned tasks, and to interact with other agents. The assigned tasks for this system are used to improve SNR according to weather's variation. These capabilities are covered by topics such as power, visibility, dust storm intensity, modulation, coding, and data rate, etc.

The system relies on satellite parameter variations, training knowledge, various problems solving, and search engines.

By implementing the core skillful optimization model as shown in Fig.7, designers are able to predict individual components of satellite networks in a cohesive manner for an enhanced DACS which will be explained in section 4.3.

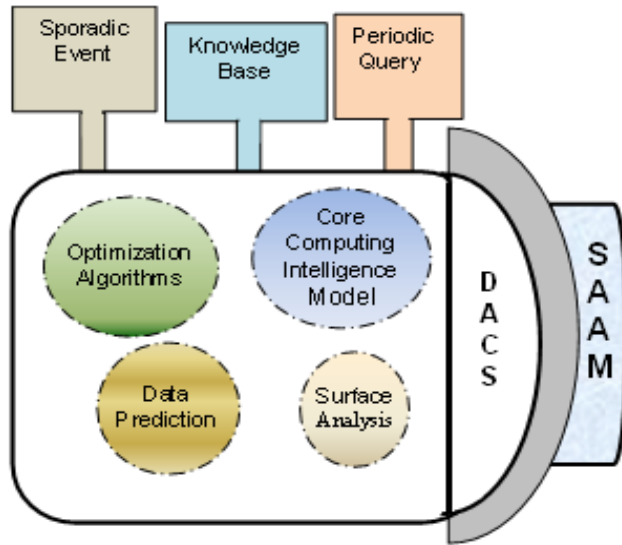


Figure 7. Network optimization decision and control system (DACS)

This high level architecture for SAAM is based on weather attenuation, dust size, power, modulation, and coding information along with other parameters. It is used to estimate the optimal decision for satellite communication systems. Such system will proficiently search for different combinations of input control variables to minimize estimated attenuation effect and maximize channel robustness and efficiency by improving SNR.

Moreover, SAAMs provide a set of efficient tools for solving problems such as wireless propagation that are impractical or difficult to solve by using traditional methods [3]. This includes heuristic search and planning algorithms, formalisms for knowledge representation, reasoning mechanisms, machine learning techniques, and methods applicable to sensing and action problems. Such methods are presented in the as variation of signal level, modulation, and coding with unpredicted weather conditions [33], [34].

4.2. Signal to Noise Ratio (SNR) Calculation

By definition, SNR is a measure of signal strength for satellite signal relative to attenuations and background noise. A better estimation for SNR values calculated under

different weather attenuations are proposed as follows:

Thermal noise power spectral density is:

$$N_0 = K \cdot T \quad (25)$$

$K = -228.6 \text{ dBWs/K}$, T (effective noise temperature) = $T_a + T_r$, where T_a noise temperature of the antenna as represented in Table 1, and

$$T_r (\text{Receiver's Noise temperature}) = \left(10^{\frac{N_r}{10}} - 1\right) \cdot 290. \quad (26)$$

Table 1. Noise Temperature in Antenna T_a (Kelvin) [35]

Antenna Noise temperature T_a (Kelvin)		
Directional satellite antenna	Earth from space	290 K
Directional terminal antenna	Space from earth at 90° elev.	3 – 10 K
	Space from earth at 10° elev.	≈ 80 K
	Sun (1...10 GHz)	$10^5 \dots 10^4 \text{ K}$
Hemispherical terminal antenna	At night	290 K
	Cloudy sky	360 K
	Clear sky with sunshine	400 K

Where noise figure of low-noise amplifier, $N_r \approx 0.7\text{--}2 \text{ dB}$. Thus, the ratio between signal and noise power spectral density is:

$$\frac{C}{N_0} = \frac{C}{K \cdot T} = \frac{P_r}{K \cdot T} = \frac{P_t \cdot G_t}{A_t} \cdot \frac{G}{K \cdot T} = \frac{EIPR}{A_t} \cdot \frac{G_r}{K \cdot T} \text{ dB}, \quad (27)$$

$$\frac{C}{N_0} = P_t + G_t - A_t + G_r - K - T \text{ dBHz}. \quad (28)$$

Where P_t and P_r are transmitted and received power. G_t and G_r are antenna gain at transmitter and receiver sides respectively. A_t (total attenuation) = A_w (atmospheric attenuation) + A_0 (free space loss). Note that, A_w is presented in (24) and A_0 will be presented in (29).

The main specification for free space attenuation is summarized by:

- Contain no electrical charge,
- Uniform everywhere,
- Carries no current, d- infinite extent in all directions

[35], [36]. Free space loss as a function of frequency is presented as:

$$A_0(f) = (4 \cdot \pi \cdot d / \lambda)^2. \quad (29)$$

Where the wavelength $\lambda = c / f$ and the distance between transmitter and receiver d is a function of the propagation angle for the line path connected between ground earth station and geosynchronous (GEO) satellite.

By considering a receive filter with noise of equivalent bandwidth B_r , the noise power N will be:

$$N_0 \cdot B_r = K \cdot T \cdot B_r, \quad (30)$$

and therefore,

$$SNR = \frac{C}{N} = \frac{C}{N_0} \cdot \frac{1}{B_r} \text{ dB}. \quad (31)$$

The SNR results, as function of frequency and propagation angle based on dust and gas attenuations, are shown in Figs. 8 and 9.

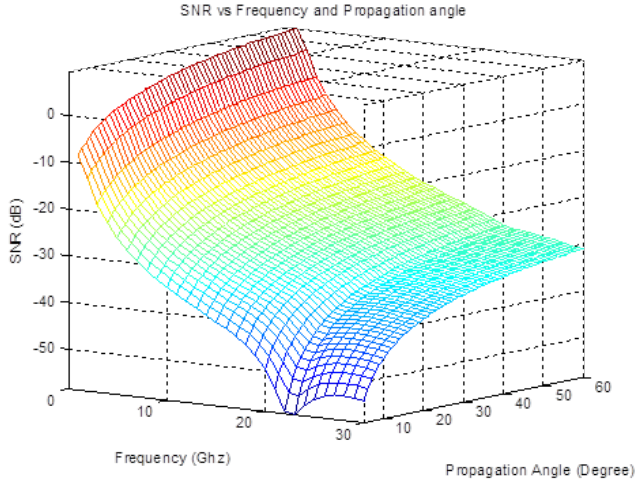


Figure 8. SNR vs. frequency and angle at KFUPM Station, Dhahran, Saudi Arabia

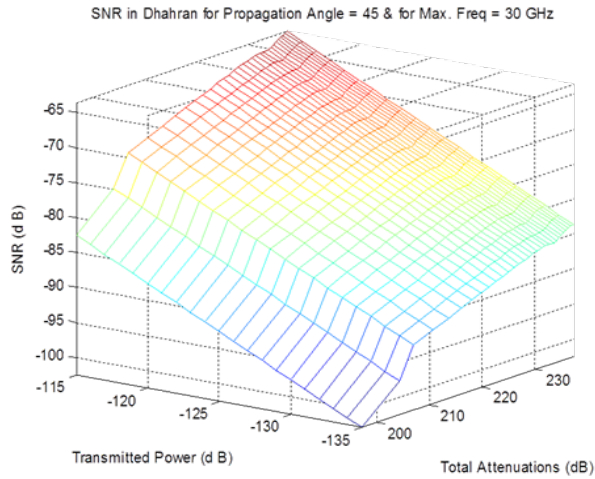


Figure 9. Output SNR at KFUPM, Dhahran station, Saudi Arabia

4.3. Decision and Control System (DACS)

The derived parameter values, being fed through SAAM to improve estimated SNR, will enable the DACS to maintain QoS and SLAs by controlling satellite signal power, frequency, modulation, coding, and data rate under unpredictable weather conditions.

The proposed method builds up a flexible SAAM based on core computing of the adaptive model that would be controlled by the predicted weather database.

Such system will proficiently search for different combinations of controlled input variables such as transmit power level, modulation schemes, channel coding rates, etc. to minimize estimated attenuation effect and maximize channel robustness and efficiency while improving SNR as shown in Fig. 10. SLA improves QoS by providing enhanced results for weather attenuations in lieu of a wide range of frequencies, visibilities, dust particular size, and propagation angles combined together. This periodically-computed attenuation will keep updating our knowledge

input to the SAAM through the gate of DACS blocks.

Real-time channel measurements such as SNR and BER can also serve as feedback tuning control to our DACS by adaptively modifying the input control variables for clear channel optimization.

4.4. Signal to Noise Ratio (SNR) Adjustment

Several factors can play an immense role in improving SNR and maximizing system throughput and availability of the link. In this section, a new proposed SAAM is introduced, as shown in Fig. 10, to overcome different weather conditions. Thus, by controlling the above mentioned factors that supply SAAM, a path is given to allow an efficient mechanism to better estimate satellite networking parameters such as link and queuing characteristics. These derived parameters would enable SAAM to maintain SNR by adaptively adjusting signal power, transmission rate, coding, and modulation under unpredictable weather conditions.

By definition, E_s (symbol energy) = $C \cdot T_s = C / R_s$, where transmission rate R_s (symbol/sec) is inversely equivalent to symbol duration T_s and energy-to-noise power density per symbol as:

$$\frac{E_s}{N_0} = \frac{C}{N_0} \cdot T_s = \frac{C}{N_0} \cdot \frac{1}{R_s}, \quad (32)$$

$$\frac{E_s}{N_0}(A_t, P_t) = P_t + G_t - A_t + G_r - T - K - R_s \text{ dB}. \quad (33)$$

This equation is used to determine bit error rate of a digital transmission system, or vice versa. Fig. 10 illustrates a manner for changing parameters of the communication system in order to overcome the deteriorating effect of atmospheric impairments, and to increase reliability of the data transmitted throughout the channel.

In the first panel, the system held signal input parameters that were compared against SNR threshold level in a single database. The results should be greater than or at least equal to this level.

In the second panel, based on SNR values, either SAAM will decide to increase transmit power up to a maximum limit of -30 dB (0 dBm) in order to reach the desired level and stop the simulation or skip to the next panel.

Next, SNR values will be checked against modulation and coding values recorded in the system. If this value can be reached by using any of the mentioned table combinations, then the system will go to the last step.

In the last step, the system will compromise among different SNR achieved outputs and make a decision based on the skilful controller according to available parameters and requirements. The given feedback will keep looping until a satisfactory value is reached.

Thus, the system has capabilities to change data rate, frame size and frequency in order to adjust SNR in cases such as unpredicted storm weather condition, by using refresh duration that is located in the first panel. However, the system has a limit of increasing the power up to -30 dB.

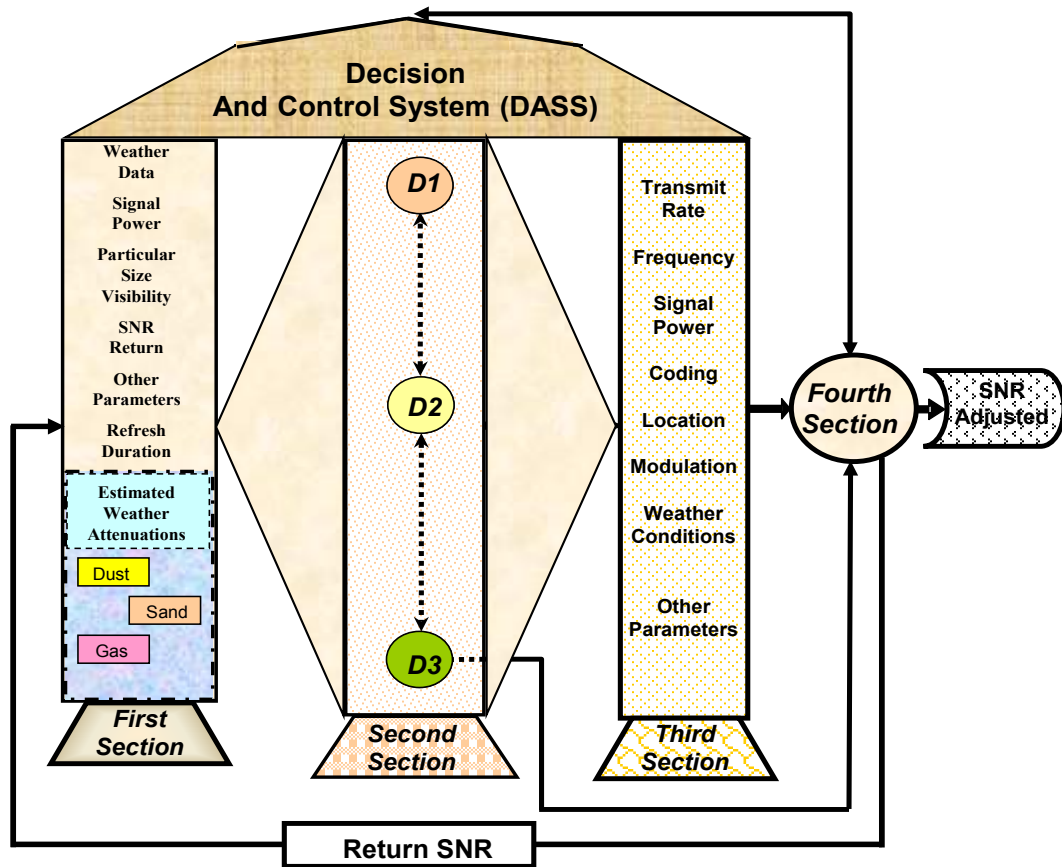


Figure 10. Skilful atmospheric aware model (SAAM) for satellite systems

Figs. 9 and 11 show a comparison for the outputs of SNR ranges before and after modification respectively. Thus, before modification, SNR fell between -102 dB and -64 dB , for power transmits from -135 dB to -115 dB , and was transformed after intelligent decision mechanism to fall within modulation and coding boundaries of allowable used database. The adjusted output for SNR ranges from -22 dB to 30 dB and -69 dB to -30 dB for transmitted power, and 197 dB to 235 dB for total attenuations in both results.

5. Simulation Results and Discussions

The predicted atmospheric attenuations were estimated, in the previous sections, at any location on earth for different operational frequency values, and for a wide range of propagation angles. These schemes provide appropriate results up to high frequency of operations as shown in Figs. 4 and 5. Moreover, these results are key factors in implementing an accurate skillful engine that would act to improve end-to-end wireless communications for different weather conditions.

This simulation pilots an enhanced back propagation - learning algorithm that is used to iteratively tune the skillful controller technique with returned SNR values for activating the weighted modulation/codepoint to its optimal value, depending on actual or predicted weather conditions,

configuration settings and tolerance or safety margins for SLAs commitment as shown in Fig. 10.

Adjusted SNR in Ottawa for Propagation Angle = 45° & Freq = 30 GHz

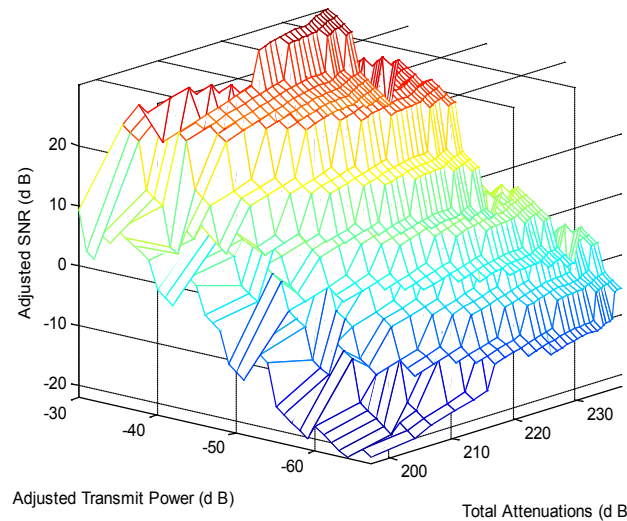


Figure 11. Output Adjusted SNR at KFUPM, Dhahran station, Saudi Arabia

Thus, the simulated SAAM checks out various combinations for different input variables based on given threshold signal level at each section and convey intelligently the ultimate value for SNR. Therefore,

the implemented skillful engine will proficiently search for the blend of available signal parameters in the presence of unpredicted channel attenuations. It will then provide us with reasonable signal recovery that satisfies at least the minimum threshold level as shown in Fig. 11.

The results are done by using MATLAB simulations, where different programs were written to collect database information from different sources such as ITU – R, to implement the three dimensional results for atmospheric attenuations, and to run the skillful engine in order to present the desired output for the communication satellite systems.

6. Conclusions

Sand, dust, gaseous, and other atmospheric properties can have a distorting effect on the QoS in satellite networks. Predicting channel attenuation due to atmospheric conditions can enable mitigation planning by adaptively selecting appropriate propagation parameters such as modulation and coding etc. This paper presented a method to estimate dust, sand, and gaseous attenuations using the signal-weather database from ITU–R propagation models combined with bi-linear interpolation, gateway, and ground terminal characteristics.

A three dimensional relationship was presented for these attenuations with both frequency and propagation angle to provide DACS with a mechanism to have an accurate view of satellite's parameters. The proposed SAAM can provide designers with a perceptible view of approximated atmospheric attenuation values by giving them the flexibility at any location to apply various combinations of modulation, coding, transmission power, and transmission rate, for all propagation angles, and for any frequency, in order to maximize satellite system's throughput and QoS for variant weather conditions. Simulation results were presented to show the effectiveness of the proposed methods.

ACKNOWLEDGEMENTS

The authors thank the EE department at KFUPM University for providing us with the full support needed for installing the satellite system equipment in order to produce the data, and for the financial support of this project.

REFERENCES

- [1] K. Harb, A. Srinivasan, B. Cheng, and C. Huang, "Prediction method to maintain QoS in weather impacted wireless and satellite networks," in Proc. SMC'07, (Montreal, QC, Canada), Oct. 2007.
- [2] K. Harb, A. Srinivasan, B. Cheng, and C. Huang, "QoS in weather impacted satellite networks," in Proc. IEEE Pacific Rim Conference on Communications, Computers and Signal Processing, (Victoria, B.C., Canada), Aug. 2007.
- [3] K. Harb, A. Srinivasan, B. Cheng, and C. Huang, "Intelligent weather aware scheme for satellite systems," in Proc. IEEE ICC'08, May 2008.
- [4] Nasa, "Hurricanes/Tropical Cyclones." Website: http://www.nasa.gov/mission_pages/hurricanes/archives/2007/hurricane_dust.html, last accessed date April 2013.
- [5] ITU–R, Propagation data and prediction method required for the design of Earth-space Telecommunication systems. Radio wave propagation, International Telecommunication Union. Rec. P.618-7, ITU–R, Fascicle, Geneva, 2001.
- [6] A. A. Aboudebra, K. Tanaka, T. Wakabayashi, S. Yamamoto, and H. Wakana, "Signal fading in land-mobile satellite communication systems: Statistical characteristics of data measured in Japan using ETS-VI," Microwave, Antennas & Propagation, vol. 146, pp. 349–354, Oct. 1999.
- [7] L. J. Ippolito and T. A. Russell, "Propagation considerations for emerging satellite communications applications," Proc. of the IEEE, vol. 81, pp. 923–929, June 1993.
- [8] V. Network, "VSAT network types." website: http://www.comsys.co.uk/wvm_mn.htm, last accessed date March 2013.
- [9] J. Goldhirsh, "Attenuation and backscatter from a derived two-dimensional dust storm model," IEEE Transactions Antennas Propagation, vol. 49, no. 12, pp. 1703–1711, 2001.
- [10] Qun-feng Dong, Ying-Le Li, Jia-dong Xu, Hui Zhang, and Ming-jun Wang, "Effect of sand and dust storms on microwave propagation," IEEE Trans. Antennas Propagation, vol. 61, no. 2, pp. 910–916, Feb. 2013.
- [11] S. O. Bashir and N. J. McEwan, "Microwave propagation in dust storms: A review," in Proc. Inst. Elect. Eng., vol. 133, pp. 241–247, June 1986.
- [12] D. G. Kaskaoutis, *Dust storm identification via satellite remote sensing*. New York: Nova Science Publishers, July 2010.
- [13] J. Goldhirsh, "A parameter review and assessment of attenuation and backscatter properties associated with dust storms over desert regions in the frequency range of 1 to 10 GHz," IEEE Trans. Antennas Propagation, vol. AP-30, pp. 1121–1127, Nov. 1982.
- [14] S. I. Ghobrial and J. A. Jervase, "Microwave propagation in dust storms at 10.5 GHz-A case study in Khartoum, Sudan," IEICE Trans. Communication, vol. E80-B, pp. 1722–1727, Nov. 1997.
- [15] S. I. Ghobrial and S. M. Sharief, "Microwave attenuation and cross polarization in dust storms," IEEE Trans. Antennas Propagation, vol. AP-35, pp. 418–425, Apr. 1987.
- [16] E. M. Patterson and D. A. Gillette, "Measurements of visibility vs. mass concentration for air-borne soil particles," Atmospheric Environment, vol. 11, no. 2, pp. 193–196, 1977.
- [17] E. A. A. Elsheikh, M. R. Islam, A. H. M. Z. Alam, A. F. Ismail, K. Al-Khateeb, and Z. Elabdin, The Effect of Particle Size Distributions on Dust Storm Attenuation Prediction for Microwave Propagation. Kuala Lumpur, Malaysia, DOI: 10.1109/ICCCE.2010.5556831, May 2010.
- [18] Z. E. O. Elshaikh, M. R. Islam, O. O. Khalifa, and H. E. Abd-El-Raouf, "Mathematical model for the prediction of microwave signal attenuation due to dust storm," Progress In

- Electromagnetics Research M, vol. 6, pp. 139–153, 2009.
- [19] Z. Elabdin and M. Islam, Duststorm Measurements for the Prediction of Attenuation on Microwave Signals in Sudan. Kuala Lumpur, Malaysia, 2008.
 - [20] E. A. A. Elsheikh, M. R. Islam, K. Al-Khateeb, A. Z. Alam, and Z. O.Elshaikh, “A proposed vertical path adjustment factor for dust storm attenuation prediction,” in 4th International Conference on Mechatronics ICOM, (Kuala Lumpur, Malaysia), May 2011.
 - [21] T. S. Chu, “Effects of sandstorms on microwave propagation,” Bell System Technology Journal, vol. 58, no. 2, pp. 549–555, 1979.
 - [22] D. G. Kaskaoutis, H. D. Kambezidis, K. V. S. Badarinath, Shailesh Kumar Kharol, *Dust Storm Identification Via Satellite Remote Sensing* (Natural Disaster Research, Prediction and Mitigation), Nova Science Publishers, Inc., New York, 2010.
 - [23] K. Harb, B. Omair, S. Abdul-Jauwad, A. Al-Yami, , and A. Al-Yami, “A proposed method for dust and sand storms effect on satellite communication networks,” in Innovations on Communication Theory INCT’12, (Istanbul, Turkey), Oct. 2012.
 - [24] D. A. Gillett, *Environmental Factors Affecting Dust Emission*, by Wind Erosion. C. Morales, Ed. New York: Wiley, 1979.
 - [25] K. Harb, F. R. Yu, P. Dakhal, and A. Srinivasan, “A decision support scheme to maintain QoS in weather impacted satellite networks,” in Proc. AIAA Atmospheric and Space Environments Conference’10, (Toronto, ON, Canada), Aug. 2010.
 - [26] ITU–R, “Attenuation by atmospheric gases,” Radio wave propagation, International Telecommunication Union Recommendation ITU–R P.676-6, 2005.
 - [27] M. Willis, “Absorption by atmospheric gases.” website: <http://www.mike-willis.com/Tutorial/gases.htm>, accessed Dec. 2012.
 - [28] K. Harb, F. R. Yu, P. Dakhal, and A. Srinivasan, “Performance improvement in satellite networks based on markovian weather prediction,” in Proc. IEEE GlobCom’10, (Miami, Florida, USA), Dec. 2010.
 - [29] R. McLeod and M. L. Baart, *Geometry and Interpolation of Curves and Surfaces*. Cambridge University Press, July 1998.
 - [30] E. G. Njoku and J. A. Kong, “Theory for passive microwave remote sensing of near surface and soil moisture,” J. Geophys. Res., vol. 82, pp. 3108–3118, 1977.
 - [31] F. E. Geiger and D. Williams, “Dielectric constants of soils at microwave frequencies,” NASA Tech. Document NASATM-X-65, 1987.
 - [32] ITU–R, Propagation data and prediction method required for the design of Earth-space Telecommunication systems. Radio wave propagation, International Telecommunication Union. Rec. P.618-7, ITU–R, Geneva, 2001.
 - [33] Y. Leung, *Intelligent spatial decision support systems*. Springer Verlag, New York, 1997.
 - [34] Telesat Canada, “ISS (Intelligent Satellite Service) Research and Development.” website: <http://www.telesat.ca>, last accessed date Feb. 2013.
 - [35] E. Lutz, M. Werner, and A. Jahn, *Satellite Systems for Personal and Broadband Communications*. Springer, New York, 2000.
 - [36] G. Maral and M. Bousquet, *Satellite Communications Systems*. John Wiley & Sons Ltd, UK, 1993.